On the stability of high-speed milling with spindle speed variation

Sébastien Seguy · Tamás Insperger · Lionel Arnaud · Gilles Dessein · Grégoire Peigné

Abstract Spindle speed variation is a well-known technique to suppress regenerative machine tool vibrations, but it is usually considered to be effective only for low spindle speeds. In this paper, the effect of spindle speed variation is analyzed in the high-speed domain for spindle speeds corresponding to the first flip (period doubling) and to the first Hopf lobes. The optimal amplitudes and frequencies of the speed modulations are computed using the semidiscretization method. It is shown that period doubling chatter can effectively be suppressed by spindle speed variation, although, the technique is not effective for the quasiperiodic chatter above the Hopf lobe. The results are verified by cutting tests. Some special cases are also discussed where the practical behavior of the system differs from the predicted one in some ways. For these cases, it is pointed out that the concept of stability is understood on the scale of the principal period of the system—that is, the speed modulation period for variable spindle speed machining and the tooth passing period for constant spindle speed machining.

Keywords Stability · Milling · Spindle speed variation · Regenerative chatter · Surface roughness

S. Seguy (✉)
INSA, UPS, Mines Albi, ISAE; ICA (Institut Clément Ader),
Université de Toulouse,
135 avenue de Rangueil,
31077 Toulouse, France
e-mail: sebastien.seguy@insa-toulouse.fr

T. Insperger
Department of Applied Mechanics,
Budapest University of Technology and Economics,
1521 Budapest, Hungary
e-mail: inspi@mm.bme.hu

L. Arnaud · G. Dessein
ENIT (École Nationale d'Ingénieurs de Tarbes),
LGP (Laboratoire Génie de Production), Université de Toulouse,
47 avenue d'Azereix, BP 1629, 65016 Tarbes Cedex, France

L. Arnaud
e-mail: lionel.arnaud@enit.fr

G. Dessein
e-mail: gilles.dessein@enit.fr

G. Peigné
Société Mitis, École Centrale de Nantes,
1 rue de la Noë,
44321 Nantes Cedex, France
e-mail: gpeigne@mitis-engineering.fr

1 Introduction

Machining by material removal is one of the most widely used manufacturing processes in the industry. The productivity of machining is often limited by vibrations that arise during the cutting process. These vibrations cause poor surface finish, increase the rate of tool wear, and reduce spindle lifetime. One reason for these vibrations is surface regeneration, i.e., the tool cuts a surface that was modulated during the previous cut. The theory of regenerative machine tool chatter is based on the works of Tobias and Fishwick [1]. This knowledge—initially dedicated to the turning process—has been adapted to milling [2, 3] and has led to the development of the stability lobe theory. Since then, several improved models and analysis techniques have appeared including detailed analysis of the governing delay differential equation and time domain simulations [4–12]. These models all use the so-called stability lobe diagrams, which make it possible to choose the maximum axial depth of cut for a given spindle speed associated with a chatter free machining. In many practical cases, however, the

choice of the optimal speed is difficult because contradictory parameters interact with productivity [13–15].

There are various ways to reduce chatter vibrations. Classical solutions are based on increasing the stiffness of the mechanical components and the damping by reducing cutting speed or by adding dampers [16]. Tools with variable pitches [17, 18] or with variable helix angles [19, 20] can also be used to suppress chatter. The idea behind these techniques is that each flute experiences different regenerative delay; in this way, the regenerative effect is disturbed and that may reduce the self-excited vibrations for certain spindle speeds.

A similar technique to disturb the regenerative effect and to suppress chatter vibrations is the spindle speed variation. As opposed to variable pitch or variable helix cutters, spindle speed variation can effectively be used in a wider spindle speed range since the frequency and the amplitude of the speed variation can easily be adjusted in CNC machines even during the machining process. The idea of spindle speed variation became the focus of interest in the 1970s. Takemura et al. [21] presented the first simple model to study the stability of variable speed machining; they predicted significant shift of the stability lobes to higher depth of cuts, but the experimental tests showed only small improvements. Sexton and Stone [22, 23] developed a more realistic model, and they found some improvements in the stability properties for low spindle speeds. Moreover, they showed that the presence of transient vibrations may further reduce these gains [24].

Stability analysis for variable speed machining requires special mathematical techniques since the corresponding mathematical model is a delayed differential equation with time-varying delay. Sexton et al. [22] considered the projection of the solutions of the system to the subspace of periodic functions and used Fourier expansion to reduce the problem to an eigenvalue analysis. Tsao et al. [25] developed a model taking the angular coordinates as variables instead of time. This approach was further improved by Jayaram et al. [26], who used a special combination of Fourier expansion and Bessel function expansion to analyze the system. Insperger and Stépán [27] used the semidiscretization method to construct stability diagrams for variable speed turning. They showed that the critical depths of cut can be increased for low speeds, but for the high-speed domain, no improvement was found. Recently, Zhang et al. [28] presents a systematic stability analysis of spindle speed variation based on a machining chatter model of nonlinear delay differential equation. Experimental validations in turning show reduction of the displacement and improvements in the surface roughness at low speed [29, 30].

The modeling of variable speed milling is more complex than that of turning since the speed variation frequency and the tooth passing frequency interact, and the resulting system is typically quasiperiodic. Still, there are mathematical techniques to determine approximate dynamic properties. Sastry et al. [31] used Fourier expansion and applied the Floquet theory to derive stability lobe diagrams for face milling. They obtained some improvements for low spindle speeds. Recently, Zatarain et al. [32] presented a general method in the frequency domain to solve the problem and show that variable spindle speed can effectively be used to chatter suppression for low cutting speeds. They used the semidiscretization method and time domain simulations to validate their model and confirmed their results by experiments. Another approach is to use time domain simulation [33, 34] that makes it possible to obtain more detailed information about the process such as the amplitude of the vibrations, the chip thickness, or the cutting forces. While theoretical results are available for a wide range of spindle speeds, to the best knowledge of the authors, experimental validations were made only for low spindle speeds [26, 29–32, 35].

In this paper, the stability of variable speed milling is analyzed in the high-speed domain for spindle speeds corresponding to the first flip (period doubling) and to the first Hopf lobes. Theoretical stability predictions are obtained using the semidiscretization method based on [36], and the results are confirmed by experiments. The structure of the paper is as follows. First, the model of the process is presented in Section 2, then, the stability properties are predicted in Section 3. The selection of the optimal amplitude and frequency is presented in Section 4. Experimental verifications are provided in Section 5. Section 6 deals with some special equivocal cases. Finally, the paper is concluded in Section 7.

2 Model of milling process with variable spindle speed

In this section, the relevant parameters of the spindle speed variation are defined, and the mechanical model of the milling process is presented.

2.1 Variation of the spindle speed

In this paper, periodic spindle speed variation is considered, i.e., the spindle speed is modulated periodically around a mean value by a given amplitude and frequency. In the literature, mostly sinusoidal, triangular or square-wave modulations are considered [21, 37]. The available frequencies and amplitudes of the modulation are limited by the spindle dynamics [33]. With the same dynamic characteristics of the spindle, the triangular modulation provides larger amplitudes and frequencies than the sinusoidal or the square-wave modulation [37]. In addition, there is no jump in speed like with a square-wave function

[37]. In the current study, the triangular variation will be analyzed.

Assume that the spindle speed variation is periodic at period, T, with a mean value, N_0, and an amplitude, N_A, that is, $N(t) = N(t+T) = N_0 + N_A S(t)$, where $S(t) = S(t+T)$ is the shape function. For a triangular modulation (see Fig. 1), the shape function is defined as:

$$S(t) = \left\{ \begin{array}{ll} 1 - 4\,\mathrm{mod}\,(t,T)/T & \text{if} \quad 0 < \mathrm{mod}(t,T) \le T/2 \\ -3 + 4\,\mathrm{mod}\,(t,T)/T & \text{if} \quad T/2 < \mathrm{mod}(t,T) \le T \end{array} \right\}. \tag{1}$$

Here, mod(t,T) denotes the modulo function, for example, mod(12, 5)=2.

According to the general notation in the corresponding literature (see, e.g., [25]), the amplitude and the frequency of the speed variation is normalized by the mean spindle speed N_0 as:

$$\mathrm{RVA} = \frac{N_A}{N_0}, \tag{2}$$

$$\mathrm{RVF} = \frac{60}{N_0 T} = \frac{60f}{N_0}. \tag{3}$$

RVA represents the ratio of the amplitude, N_A, and the mean value, N_0. In practical applications, the maximum value for RVA is about 0.3. This represents a variation of 30% of the spindle speed and results in a variation of 30% of the feed by tooth due to the constant feed velocity. RVF is the ratio of the variation frequency, f, and the average spindle frequency, N_0/60. The variation frequency, f, is typically about 1–2 Hz.

Using the normalized parameters introduced above, the triangular modulation can be given as:

$$N(t) = \left\{ \begin{array}{ll} N_0(1 + RVA) - \dfrac{4N_0\,RVA}{T}\,\mathrm{mod}\,(t,T) & \text{if} \quad 0 < \mathrm{mod}(t,T) \le T/2 \\ N_0(1 - 3RVA) + \dfrac{4N_0\,RVA}{T}\,\mathrm{mod}\,(t,T) & \text{if} \quad T/2 < \mathrm{mod}(t,T) \le T \end{array} \right\}. \tag{4}$$

The time delay between two subsequent cutting teeth plays a crucial role in the dynamics of the system due to the

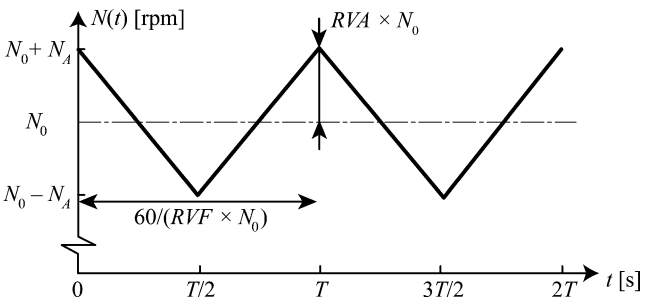

Fig. 1 Typical triangular shape variation

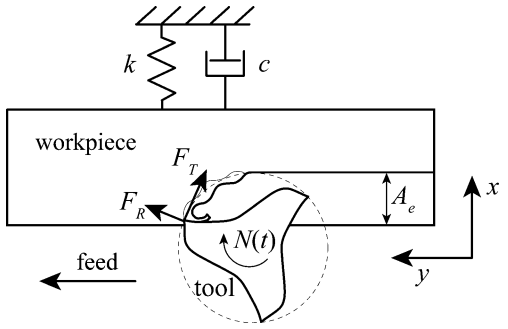

Fig. 2 Mechanical model of the milling process with single degree of freedom

regenerative effect. For a machining process with constant spindle speed, N_0, this time delay is constant:

$$\tau_0 = \frac{60}{zN_0}, \tag{5}$$

where z is the number of the teeth of the tool. For variable spindle speed machining, the time delay varies periodically in time according to the spindle speed modulation. The variation of the regenerative delay can be given in the implicit form:

$$\int_{t-\tau(t)}^{t} \frac{N(s)}{60}\,\mathrm{d}s = \frac{1}{z}. \tag{6}$$

For the triangular modulation defined in Eq. 4, this equation gives:

$$\tau(t) = \left\{ \begin{array}{ll} \tau_0(1 - RVA) + \dfrac{4\tau_0\,RVA}{T}\,\mathrm{mod}\,(t,T) & \text{if} \quad 0 < \mathrm{mod}(t,T) \le T/2 \\ \tau_0(1 + 3RVA) - \dfrac{4\tau_0\,RVA}{T}\,\mathrm{mod}\,(t,T) & \text{if} \quad T/2 < \mathrm{mod}(t,T) \le T \end{array} \right\}, \tag{7}$$

where τ_0 is the mean time delay.

2.2 Mechanical model

A schematic diagram of the milling process is shown in Fig. 2. The structure is assumed to be flexible in the x direction, while the feed is parallel to the y direction. The dynamic model is defined by the following equation:

$$m\,\ddot{x}(t) + c\,\dot{x}(t) + kx(t) = F_x(t), \tag{8}$$

where m is the modal mass, c is the damping, k is the stiffness, and $F_x(t)$ is the cutting force in the x direction. According to the linear cutting law, the x component of the force is given by:

$$F_x(t) = A_\mathrm{p} \sum_{j=1}^{z} \left[\left(K_\mathrm{R} \cos\varphi_j - K_\mathrm{T} \sin\varphi_j \right) h_j(t) \right], \tag{9}$$

where A_p is the axial depth of cut, φ_j is the angular position of the jth cutting edge, and K_T and K_R are the specific

tangential and radial cutting coefficients. The chip thickness is expressed by:

$$h_j(t) = g_j(t)\Big(f_z \sin\varphi_j + [x(t) - x(t-\tau(t))]\cos\varphi_j\Big), \qquad (10)$$

where the function $g_j(t)$ is a unit function, which is equal to 1 when the jth tooth is cutting; otherwise, it is equal to 0. Here, f_z is the feed per tooth, $x(t)$ is the current position of the tool, and $x(t\text{-}\tau(t))$ is the position at the previous cut. The regenerative delay $\tau(t)$ is periodic in time due to the spindle speed modulation, as it is given in Eq. 7.

3 Theoretical stability predictions

Stability of the variable speed machining is predicted using the semidiscretization method based on [27] and [36]. This method can be used to derive stability charts for delayed systems with time-periodic coefficients and with time-periodic delay as shown in [36]. The semidiscretization method was already used for milling models with varying regenerative delays in [38] and [39]; however, in these models, the spindle speed was constant, and the variation of the delay arose due to the accurate modeling of the feed motion.

In order to verify the results obtained by semidiscretization, the system's behavior is determined as well by time domain simulations for some spindle speeds. The results obtained by the two methods are compared for both constant and variable spindle speeds.

3.1 Stability analysis by semidiscretization

Equations 8, 9, and 10 imply the time-periodic delay differential equation in the form:

$$\begin{aligned} \dot{\mathbf{x}}(t) &= \mathbf{A}(t)\mathbf{x}(t) + \mathbf{B}(t)\mathbf{u}(t-\tau(t)), \\ \mathbf{u}(t-\tau(t)) &= \mathbf{C}\mathbf{x}(t-\tau(t)), \end{aligned} \qquad (11)$$

where

$$\mathbf{x}(t) = \begin{bmatrix} x(t) \\ \dot{x}(t) \end{bmatrix}, \quad \mathbf{A}(t) = \begin{bmatrix} 0 & 1 \\ v(t) - \frac{k}{m} & -\frac{c}{m} \end{bmatrix}, \quad \mathbf{B}(t) = \begin{bmatrix} 0 \\ v(t) \end{bmatrix},$$
$$\mathbf{u}(t-\tau(t)) = [x(t-\tau(t))], \quad \mathbf{C} = [\,1 \quad 0\,], \qquad (12)$$

with

$$v(t) = \frac{A_p}{m}\left(\sum_{j=1}^{z} g_j(t)\Big[K_R\cos\varphi_j - K_T\sin\varphi_j\Big]\cos\varphi_j\right). \qquad (13)$$

As shown by Eq. 7, the regenerative time delay is periodic at the spindle modulation period T. We assume that the ratio of the modulation period T and the mean time delay τ_0 is a rational number, i.e., $qT=p\tau_0$ with q and p being relative primes. Thus, the system is periodic at the principal period qT, consequently, the Floquet theory of periodic DDEs can be applied. Note that if the ratio of T and τ_0 is not rational, then the system is quasiperiodic, and the Floquet theory cannot be used.

Stability is determined using the first-order semidiscretization method according to [40]. The scheme of the approximation is shown in Fig. 3. First, the discrete time scale $t_i=i\Delta t$, $i=0,1,2,...$ is introduced so that $qT=K\Delta t$ with K being an integer. In the ith discretization interval, the time delay is approximated by its integral average as:

$$\tau_i \approx \frac{1}{\Delta t}\int_{t_i}^{t_{i+1}} \tau(s)ds, \qquad t \in [t_i, t_{i+1}]. \qquad (14)$$

Then, the delayed term $\mathbf{u}(t\text{-}\tau(t))$ is approximated by the linear function of time as

$$\begin{aligned} \mathbf{u}(t-\tau(t)) \approx \mathbf{u}(t-\tau_i) \approx & \frac{t-\tau_i-t_{i-r_i}}{\Delta t}\mathbf{u}_{i+1-r_i} \\ & + \frac{t_{i+1-r_i}+\tau_i-t}{\Delta t}\mathbf{u}_{i-r_i}, \\ & t \in [t_i, t_{i+1}], \end{aligned} \qquad (15)$$

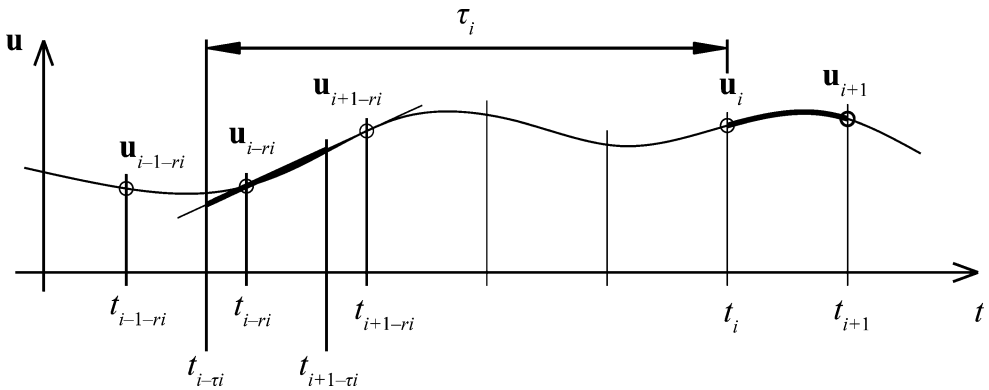

Fig. 3 Schematic diagram of the semidiscretization method

where

$$r_i = \mathrm{int}\left(\frac{\tau_i}{\Delta t} + \frac{1}{2}\right), \tag{16}$$

and $\mathbf{u}_i = \mathbf{u}(t_i)$ is used as short notation. Note that $r_i \Delta t$ is a kind of integer approximation of the delay, τ_i. Finally, the time-periodic functions are approximated by their integral average:

$$\mathbf{A}_i = \frac{1}{\Delta t}\int_{t_i}^{t_{i+1}} \mathbf{A}(s)ds, \qquad \mathbf{B}_i = \frac{1}{\Delta t}\int_{t_i}^{t_{i+1}} \mathbf{B}(s)ds, \qquad t \in [t_i, t_{i+1}]. \tag{17}$$

Now, the equation of motion 11 is approximated by:

$$\dot{\mathbf{x}}(t) = \mathbf{A}_i\mathbf{x}(t) + \mathbf{B}_i\left(\frac{t - \tau_i - t_{i-r_i}}{\Delta t}\mathbf{u}_{i+1-r_i} + \frac{t_{i+1-r_i} + \tau_i - t}{\Delta t}\mathbf{u}_{i-r_i}\right), \quad t \in [t_i, t_{i+1}]. \tag{18}$$

In each discretization interval, this system can be considered as an ordinary differential equation with a forcing term, which linearly depends on time. Thus, if $\mathbf{x}_i = \mathbf{x}(t_i)$, $\mathbf{u}_{i+1-r_i} = \mathbf{u}(t_{i+1-r_i})$, $\mathbf{u}_{i-r_i} = \mathbf{u}(t_{i-r_i})$ are given, then the solution over the interval $t \in [t_i, t_{i+1}]$ can be constructed analytically as:

$$\mathbf{x}_{i+1} = \mathbf{x}(t_{i+1}) = \mathbf{P}_i\mathbf{x}_i + \mathbf{R}_{i0}\mathbf{u}_{i-r_i} + \mathbf{R}_{i1}\mathbf{u}_{i+1-r_i}, \tag{19}$$

where

$$\begin{aligned}
\mathbf{P}_i &= \exp(\mathbf{A}_i\Delta t),\\
\mathbf{R}_{i0} &= \left(\mathbf{A}_i^2 + \tfrac{1}{\Delta t}\mathbf{A}_i^{-2}(\mathbf{I} - \exp(\mathbf{A}_i\Delta t)) - \tfrac{\tau_i - (1+r)\Delta t}{\Delta t}\mathbf{A}_i^{-1}(\mathbf{I} - \exp(\mathbf{A}_i\Delta t))\right)\mathbf{B}_i,\\
\mathbf{R}_{i1} &= \left(-\mathbf{A}_i^{-1} + \tfrac{1}{\Delta t}\mathbf{A}_i^{-2}(\mathbf{I} - \exp(\mathbf{A}_i\Delta t)) - \tfrac{r\Delta t - \tau_i}{\Delta t}\mathbf{A}_i^{-1}(\mathbf{I} - \exp(\mathbf{A}_i\Delta t))\right)\mathbf{B}_i.
\end{aligned} \tag{20}$$

Here, $\mathbf{I}$ denotes the 2×2 unit matrix. This solution can be represented by a discrete map

$$\mathbf{y}_{i+1} = \mathbf{Q}_i\mathbf{y}_i, \tag{21}$$

with

$$\mathbf{y}_i = \begin{bmatrix} \mathbf{x}_i \\ \mathbf{u}_{i-1} \\ \mathbf{u}_{i-2} \\ \vdots \\ \mathbf{u}_{i-r_{\max}} \end{bmatrix},$$

$$\mathbf{Q}_i = \begin{bmatrix}
\mathbf{P}_i & \mathbf{0} & \mathbf{0} & \cdots & \mathbf{0} & \mathbf{R}_{i1} & \mathbf{R}_{i0} & \mathbf{0} & \cdots & \mathbf{0} & \mathbf{0} \\
\mathbf{C} & \mathbf{0} & \mathbf{0} & \cdots & \mathbf{0} & \mathbf{0} & \mathbf{0} & \mathbf{0} & \cdots & \mathbf{0} & \mathbf{0} \\
\mathbf{0} & \mathbf{I} & \mathbf{0} & \cdots & \mathbf{0} & \mathbf{0} & \mathbf{0} & \mathbf{0} & \cdots & \mathbf{0} & \mathbf{0} \\
\vdots & & \ddots & & \vdots & \vdots & \vdots & \vdots & & \vdots & \vdots \\
\mathbf{0} & \mathbf{0} & \mathbf{0} & \ddots & \mathbf{0} & \mathbf{0} & \mathbf{0} & \mathbf{0} & \cdots & \mathbf{0} & \mathbf{0} \\
\mathbf{0} & \mathbf{0} & \mathbf{0} & & \mathbf{I} & \mathbf{0} & \mathbf{0} & \mathbf{0} & \cdots & \mathbf{0} & \mathbf{0} \\
\mathbf{0} & \mathbf{0} & \mathbf{0} & \cdots & \mathbf{0} & \mathbf{I} & \mathbf{0} & \mathbf{0} & \cdots & \mathbf{0} & \mathbf{0} \\
\mathbf{0} & \mathbf{0} & \mathbf{0} & \cdots & \mathbf{0} & \mathbf{0} & \mathbf{I} & \mathbf{0} & \cdots & \mathbf{0} & \mathbf{0} \\
\vdots & \vdots & \vdots & & \vdots & \vdots & & \ddots & & \vdots & \vdots \\
\mathbf{0} & \mathbf{0} & \mathbf{0} & \cdots & \mathbf{0} & \mathbf{0} & \mathbf{0} & \mathbf{0} & \ddots & \mathbf{0} & \mathbf{0} \\
\mathbf{0} & \mathbf{0} & \mathbf{0} & \cdots & \mathbf{0} & \mathbf{0} & \mathbf{0} & \mathbf{0} & & \mathbf{I} & \mathbf{0}
\end{bmatrix}, \tag{22}$$

where $\mathbf{R}_{i1}$ and $\mathbf{R}_{i0}$ are in the $(r_i\text{-}1)$th and the r_ith column of the matrix and $r_{\max} = \max(r_0, r_1, \ldots r_{K\text{-}1})$. Note, that in this case, the elements $\mathbf{u}_i$ are 1×1 matrixes, and the corresponding 1×1 unit matrixes $\mathbf{I}$ below the diagonal are in fact the scalar unit 1.

The approximate Floquet transition matrix can be given after computing matrix $\mathbf{Q}_i$ in K succeeding discretization intervals:

$$\mathbf{\Phi} = \mathbf{Q}_{K-1}\mathbf{Q}_{K-2}\ldots\mathbf{Q}_0. \tag{23}$$

If the eigenvalues of $\mathbf{\Phi}$ are in modulus less than 1, then the process is stable. Stability lobes can be constructed by scanning the cutting conditions (spindle speed and axial depth of cut) for a couple of (RVA and RVF) parameters.

3.2 Time domain simulation

The solution of the system described by Eqs. 8, 9, and 10 can be approximated by standard time domain simulation techniques, see e.g., [4, 7, 10, 33]. In this paper, the Newmark integration scheme is used with average acceleration [10]. The spindle speed variation is taken into account by adjusting the time step so that the angular step is kept constant during the simulation. This way, the position at the previous cut can be computed easily. The nonlinearity due to the exit from the cut is taken into account, thus, the displacement of motion reaches its limits even for strong vibrations.

Time domain simulation gives information about the history of the vibrations during machining. The stability of the process can be detected by monitoring the peak-to-peak amplitude of displacement [4, 33].

3.3 Verification of the predicted stability for constant spindle speed

First, the stability chart for a constant spindle speed process is determined using the semidiscretization method, then, time domain simulations are used to verify the results. The parameters of the system are collected in Table 1. The results are presented in Fig. 4. Panel (a) shows the stability lobes obtained by the semidiscretization, while panels (b), (c), (d), and (e) show the evolution of the peak-to-peak displacements obtained by time domain simulation for four specific speeds also denoted in panel (a). In panels (b) and (d), the vibration amplitudes can be seen to increase almost linearly with the axial depth of cut. These cases are

Table 1 First-order modal parameters and cutting force coefficients

m(kg)	f_1(Hz)	ξ(%)	K_T(MPa)	K_R(MPa)
1.637	222.5	0.50	700	140

associated with stable machining where the amplitude of the forced vibrations increases almost linearly with the amplitude of the cutting force. Panels (c) and (e) show that after a linear part, there is an abrupt change in the amplitudes. This corresponds to the onset of chatter at the critical depth of cut that corresponds closely to the predictions in panel (a).

Note that the spindle speed corresponding to the tooth passing frequency is 60 f_1 / z=4,450 rpm (where f_1= 222.5 Hz, and the number of teeth is z=3). Thus, the lobes presented in Fig. 4. are the first Hopf and the first flip lobes.

3.4 Verification of the predicted stability for variable spindle speed

In the same way, the two approaches were compared for variable spindle speed. Parameters RVA and RVF were fixed at 0.3 and 0.003, respectively. The results are presented in Fig. 5. Panel (f) shows the stability lobes obtained by the semidiscretization method, panels (g), (h), (i), and (j) show the peak-to-peak displacements obtained by time domain simulations for four specific spindle speeds. These latter plots show that a smooth increase in the amplitudes is followed by an abrupt change at a specific depth of cut denoting the onset of chatter. This behavior corresponds to the stability lobes in panel (f). In panel (j), the critical depth of cut is about 2.5 mm, whereas, the lobe in panel (f) gives a value of 3 mm. This slight difference could be explained by the limited number of periods taken into account in the time domain simulation.

Thus, the stability prediction for variable spindle speed milling obtained by semidiscretization is confirmed by time domain simulations. In the next sections, only semidiscretization will be used to determine optimal parameters with chatter free machining since the corresponding stability computation is much faster in time than it is with time domain simulation.

For comparison, Fig. 5 (f) also presents the lobes for constant spindle speed. The critical depth of cut can be seen to be increased by speed variation for some ranges of spindle speeds, but for some other ranges, the critical depth of cut is less than that of the constant spindle speed. For example, a cutting process with an axial depth of cut of 2 mm and a spindle speed of 9,100 rpm—that is unstable for constant spindle speed—can be stabilized by a speed variation. In contrast, at 8,900 rpm stable machining can be destabilized by a variable spindle speed. Overall, the critical depth of cut can be seen to be increased essentially in the area of the first flip lobe by spindle speed variation, as experiments too will confirm.

4 Selection of the optimal parameters

Stability of variable speed machining is very sensitive to the choice of the frequency and amplitude parameters. In

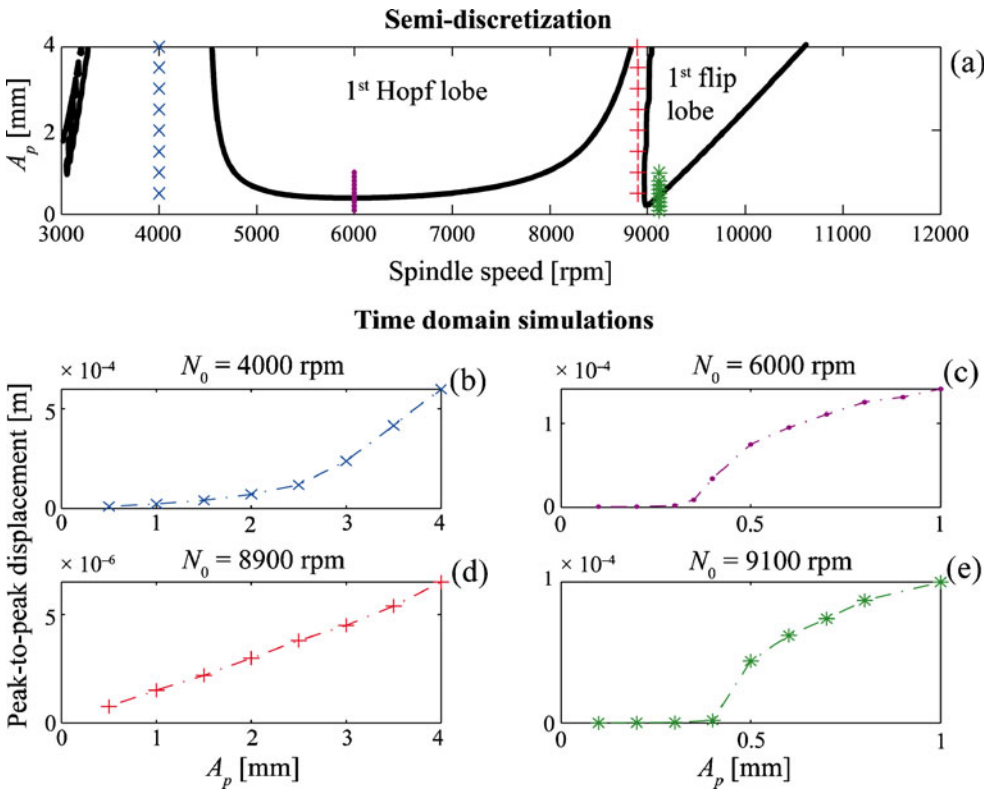

Fig. 4 Comparison of semidiscretization and time domain simulations for constant spindle speed

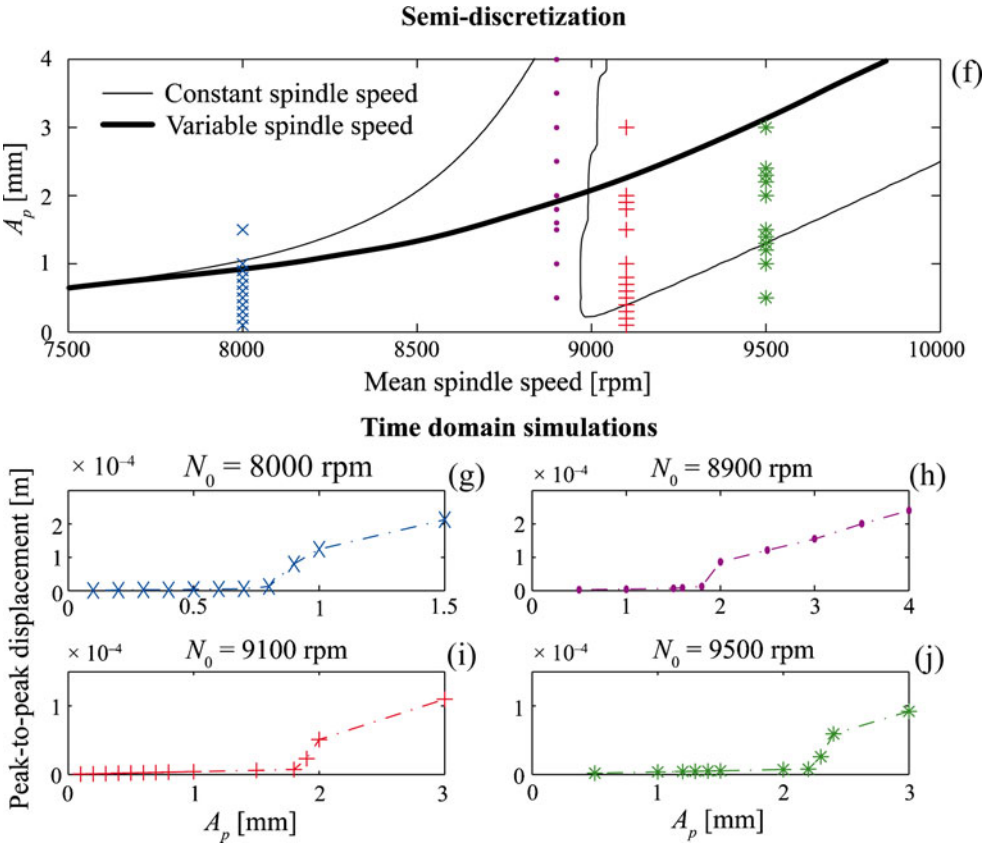

Fig. 5 Comparison of semi-discretization and time domain simulations for variable speed with RVA=0.3 and RVF=0.003

order to find the optimal modulation, different combinations of frequencies and amplitudes should be analyzed. Here, the effectiveness of the spindle speed variation is investigated in the area of the first flip lobe (N_0=9,100 rpm) and also in the area of the first Hopf lobe (N_0=8,900 rpm). For these spindle speeds, the critical depths of cut were determined for several modulation amplitudes (RVA) and frequencies using the semidiscretization method. The results for an average spindle speed of 9,100 rpm are presented in Fig. 6 in contour plot form. The diagram was constructed by computing the critical depth of cut over a 40×40 sized grid of frequency and amplitude parameters. A perfectly uniform grid is obtained here by using rational numbers (see Section 3.1). For constant speed, the critical depth of cut is 0.5 mm. For variable spindle speed, the critical depth of cut A_p is always greater than 0.5 mm for any RVA and RVF values. For some domains, even A_p= 2.4 mm can be achieved corresponding to a 380% increase

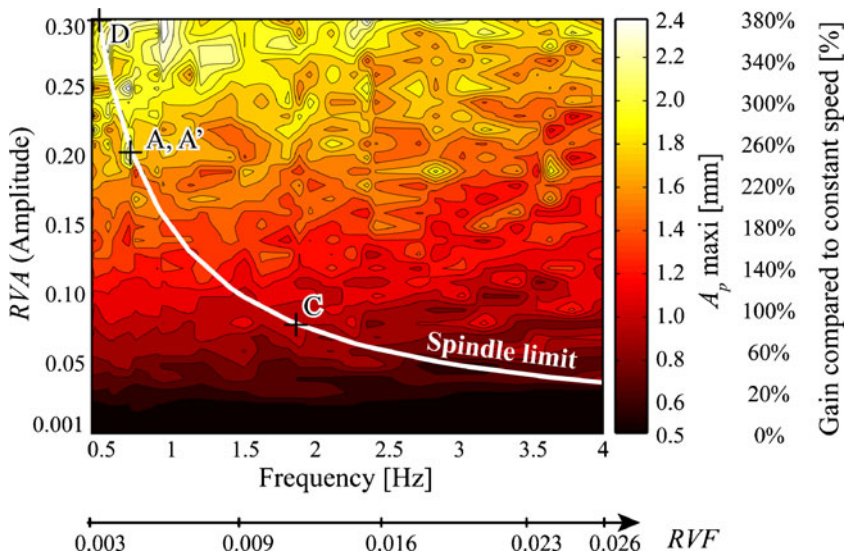

Fig. 6 Parametric study for N_0=9,100 rpm and A_e=2 mm

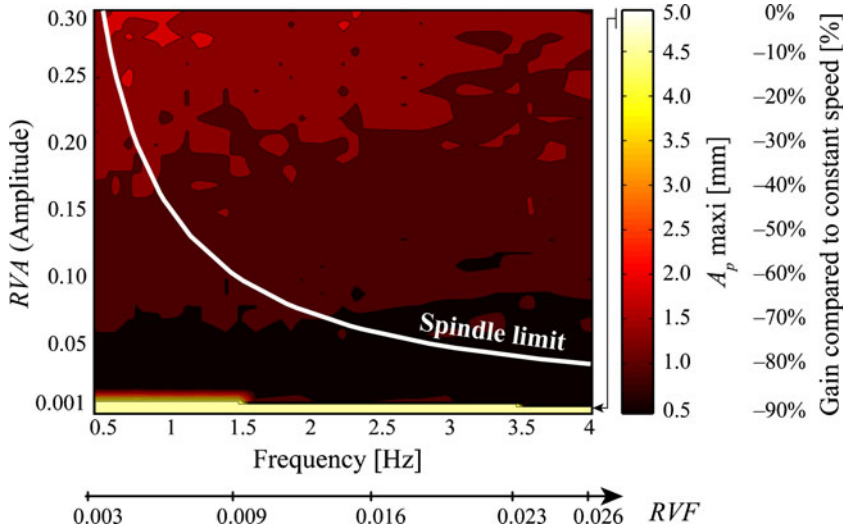

Fig. 7 Parametric study for N_0=8,900 rpm and A_e=2 mm

in the depth of cut. Figure 6 also shows that a wide frequency of speed variation coupled with low amplitude does not produce any gain in the depth of cut. The most effective parameter is amplitude variation, while the frequency does not have a significant effect on the stability within the range of 0.5–4 Hz. As mentioned earlier, the choice of the frequency and the amplitude variation is limited by the spindle dynamics. Within the range of variation, the maximum acceleration of the spindle is 100 rev/s^2, i.e., 6,000 rpm/s. For a triangular shape variation, this limit is basically determined by the maximum acceleration of the spindle:

$$a_{\max} = \frac{4 \times \mathrm{RVA} \times N_0 \times f}{60} = 100 \text{ rev/s}^2. \quad (24)$$

This limit gives a hyperbola in the frequency–amplitude diagram (see Fig. 6). Considering this limit, the optimal choice is to apply a low frequency of modulation with wide amplitude. Such cases are denoted by points A and D.

Figure 7 shows a similar contour plot for an average spindle speed of 8,900 rpm. At constant spindle speed, the maximum depth of cut is 5 mm. It can be noted that for variable spindle speed, the critical depth of cut never exceeds 5 mm for any frequencies and amplitudes. Thus, in this case, the application of speed variation always reduces the critical depth of cut. The greatest critical depth of cut is obtained for the borderline case when the amplitude tends towards zero, i.e., for the limit case of constant spindle.

Based on the above numerical studies, it can be concluded that the efficiency of spindle speed variation in high-speed milling is diverse for different spindle speeds. For the area of the first flip lobe, the critical depth of cut can essentially be increased as shown in Fig. 6. However, for the area of the first Hopf lobe, no significant gains in the depth of cut can be achieved by spindle speed variation. Furthermore, the improvements were found to depend mostly on the amplitude of the speed variation, and dependence on frequency is low.

5 Experimental work

The machining tests were carried out on a high-speed milling center (Huron, KX10). The average feed per tooth was 0.1 mm/tooth. The tool was an inserted mill with three teeth, D=25 mm, diameter without helix angle. The spindle speed variation was implemented by a subprogram using a synchronous function (Siemens, 840D). In compliance with the dynamics of the spindle, the difference between the input and the measured spindle speed trajectory was less than 0.5% (see Fig. 8). According to manufacturers of spindles and power controllers, the life span of neither the spindle nor the controller should be shortened by spindle speed variation.

The setup of the milling tests can be seen in Fig. 9. A flexure was used to provide a single degree of freedom system that is compliant in the x direction (perpendicular to the feed). The tool is considered to be rigid compared to the

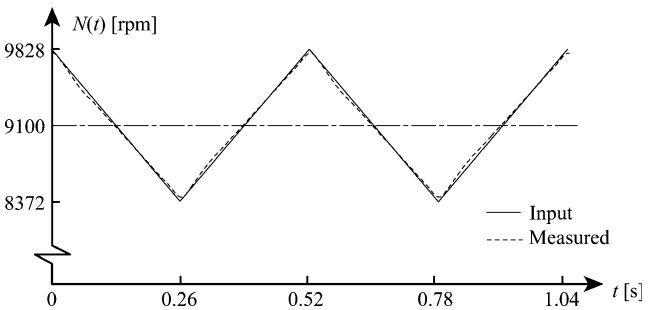

Fig. 8 Comparison between input and measured spindle speed trajectory, for N_0=9,100 rpm; RVA=0.08; and RVF=0.0125 (f= 1.9 Hz)

Fig. 9 Experimental setup

flexure. An aluminum (2017A) part was down milled with a radial depth of cut A_e=2 mm, thus, the radial immersion ratio was A_e/D=0.08. The length of the workpiece was 90 mm, and the operation time was approximately 2 s at a spindle speed of 9,100 rpm. The vibrations of the part were measured by a laser velocimeter (Ometron, VH300+). Filtering followed by a numerical integration was used to extract vibrating displacement of the part.

The dynamic characteristics of the system were determined by hammer impact test [41]. The modal parameters and the cutting force coefficients are collected in Table 1 in Section 3. The cutting force coefficients were determined in coherence with previous work [13].

5.1 Constant spindle speed tests

First, a series of tests at a constant speed has been conducted in order to verify the model. The results are shown in Fig. 10. Stable cutting tests are labeled by circle while unstable tests by crosses. The predicted behavior of the system corresponds to the experiments. The zone of period doubling chatter at the first flip lobe is also explored using a finer spindle speed resolution.

5.2 Stabilization via spindle speed variation

In this section, chatter suppression by spindle speed variation is presented by an example. Consider the machining process with spindle speed of 9,100 rpm and depth of cut of 1 mm. For constant spindle speed, this process is unstable (see Fig. 5). Spindle speed variation is applied according to point A in Fig. 6. The corresponding parameters are RVA=0.2 and RVF=0.0046875 (f= 0.71 Hz). Based on the theoretical predictions in Fig. 6, the critical depth of cut is about 2 mm, i.e., the system with variable spindle speed is predicted to be stable. The experimental results are presented in Fig. 11. Test (A) refers to the variable speed machining, and test (B) refers to the constant spindle speed machining. Figure 11 presents the spindle speed, displacement history, and surface roughness for both cases.

For an ideally symmetric tool, the pitch of the machined profile is equal to the feed per tooth. However, if the tool has a runout greater than the roughness of the surface, then it leaves only one mark per revolution. The tool used in the tests had a runout of 10 μm, the feed per tooth was 0.1 mm, and the tool had three teeth; thus, the pitch of the machined profile is expected to be approximately 0.3 mm for stable machining. (In fact, the pitch varies slightly around 0.3 mm, since the constant feed velocity and the variable spindle speed produce a varying feed per tooth.)

During the tests with variable spindle speed, no chatter was observed. The amplitude of the vibrations was less than 0.01 mm, the roughness was 1.75 μm, and the pitch of the machined profile was 0.3 mm as it can be seen in Fig. 11. These all refer to a stable cutting process.

For constant spindle speed, chatter was clearly identified. The amplitude of the vibrations was about 0.07 mm, the roughness was 3.7 μm, and the pitch of the machined profile was 0.6 mm that refers to the period doubling chatter (note that these cutting parameters are in the first flip lobe, see point B in Fig. 10).

In these cases, identification of chatter was unambiguous, the pitches of the machined profiles were uniform all along the workpiece. However, there are some cases where the stability of the process cannot be clearly assessed as will be shown in the next sections.

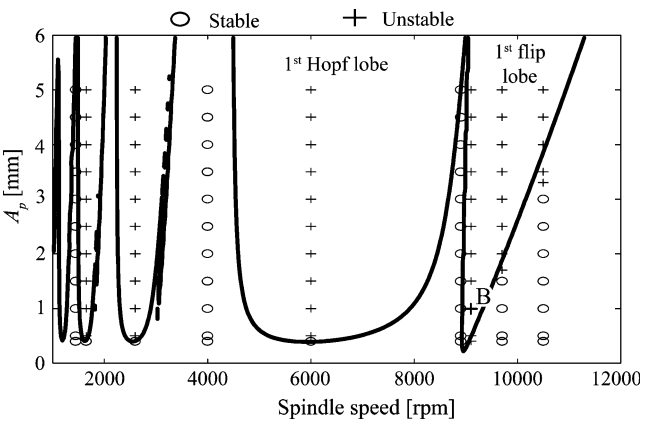

Fig. 10 Experimental test at constant spindle speed

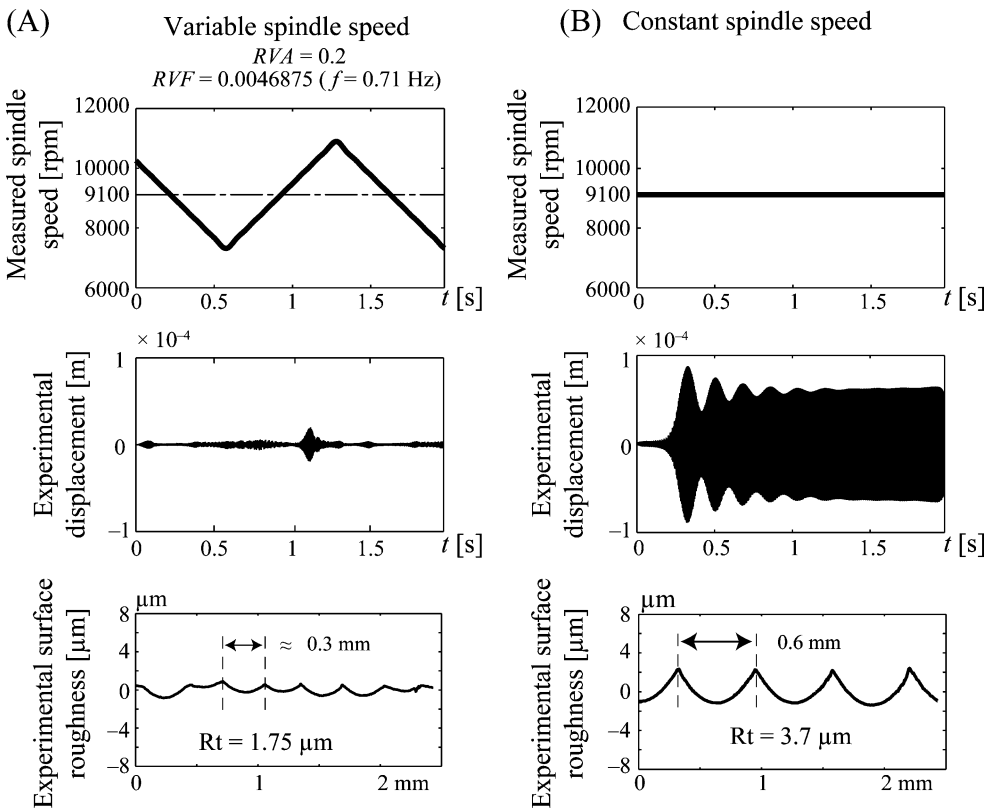

Fig. 11 Chatter suppression by spindle speed variation for A_p= 1 mm and N_0=9,100 rpm

6 Some equivocal cases

The stability of the machining process with spindle speed variation is not always as univocal as it was shown in the previous section. An unstable machining process with slowly increasing vibration amplitudes can be acceptable for a short machining process if chatter does not develop by the end of machining. Similarly, a stable process with strong transient vibrations is undesirable. In the following subsections, cutting tests for these two cases will be presented.

6.1 Globally unstable, but "practically stable" machining

Cutting tests were performed at spindle speed of 9,100 rpm and depth of cut of 1 mm using variable spindle speed with RVA=0.08 and RVF=0.0125 (f=1.9 Hz). This variation corresponds to point C in Fig. 6. Based on the theoretical predictions, the critical depth of cut is about 0.8 mm, i.e., the process is unstable. Figure 12 shows the recorded displacement history and the surface roughness variation during the cutting process. After about two periods of speed variation, the amplitude of the displacement increases very strongly. The envelope curve of the vibrations is illustrated by dashed lines in Fig. 12. This behavior corresponds to the predicted instability. However, chatter does not appear suddenly—some time is needed for it to fully develop. In the case of the cutting test in Fig. 12, this time span is about 0.7 s. If the duration of the machining process is less than this period, then large amplitude vibrations do not develop. In a sense, this case can be considered as "practically stable" machining in spite of the fact that the process itself is globally unstable. If the duration of the machining process is longer, then chatter develops.

This effect can also be observed on the surface roughness of the workpiece (see Fig. 12). The left hand side of the machined profile, where the cutting was started, has a pitch of approximately 0.3 mm with roughness of 1.6 μm. For a three fluted tool with runout of 10 μm and feed per tooth 0.1 mm, this corresponds to stable machining. As the tool passes over and chatter develops, the surface roughness gets worse and worst. By the end of the workpiece, the roughness increased to 13.9 μm. Here, the pitch is determined mainly by the vibrations of the workpiece and the sign of the feed per tooth cannot be detected on the surface.

6.2 Globally stable, but "practically unstable" machining

Cutting tests were performed at spindle speed of 9,100 rpm and depth of cut of 2 mm using variable spindle speed according to points D and A' in Fig. 6. The critical depth of cuts for point A' is 2.1 mm and for point D is 2.2 mm, thus, both cases result in stable machining, but they are close to

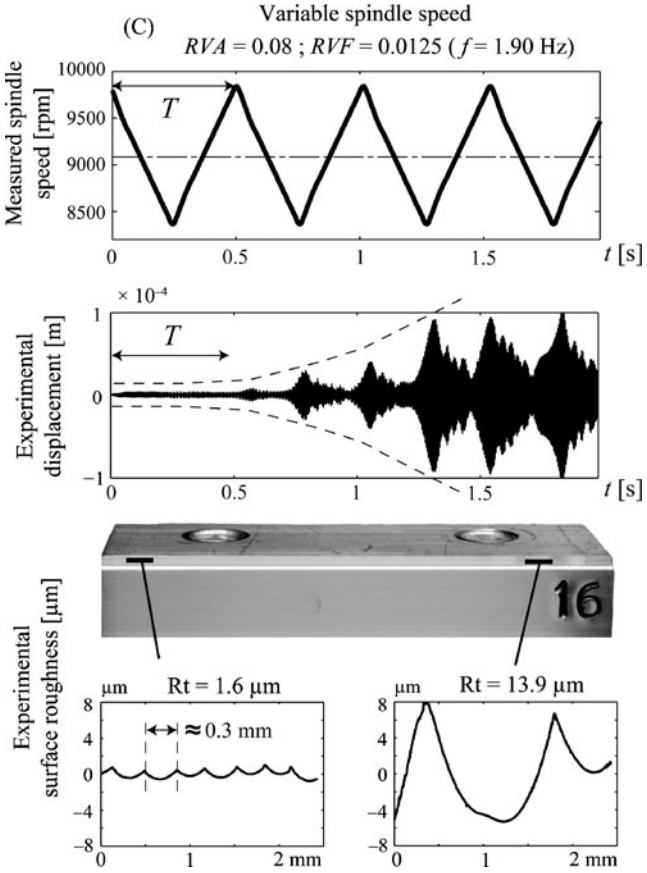

Fig. 12 Analysis of an unstable machining for A_p=1 mm and N_0= 9,100 rpm

the stability boundary. The recorded displacement history and the surface roughness variation during the cutting process are presented in Fig. 13.

Test (D) presents a strong transient vibration that slowly decays in time. Although, this is a stable machining, the heavy transient vibrations degrade the surface roughness. The rate of decay of the vibrations is low since the system is close to the stability boundary. In this case, the operation time (2 s) to machine the workpiece (length 90 mm) was less than the spindle variation period $T=1/f=2.22$ s.

For test (A'), a lower amplitude was applied allowing a higher modulation frequency of 0.71 Hz that corresponds to the spindle variation period $T=1/f=1.41$ s. Similar to case (D), strong transient vibrations arise in the first period of the variation degrading the surface roughness. However, as clearly seen in Fig. 13, the magnitude of these vibrations decreases for the second period of the variation.

The conclusion drawn from cutting tests (D) and (A') is that, although these cases correspond to a theoretically stable machining process, heavy transient vibrations arise and decay only after 1–2 periods of speed variation. Thus, these cases can be called "practically unstable," in spite of the fact that the process itself is globally stable. One reason for the slow decay of the transient vibrations is that tests (D) and (A') are close to the stability boundary, and the eigenvalues of the Floquet transition matrix are close to one. Another reason is that the decay time of the transient vibrations is scaled to the principal period qT of the system (with T being the speed variation period, see the explanation after Eq. 13), which is relatively high compared to the tooth passing period, τ_0.

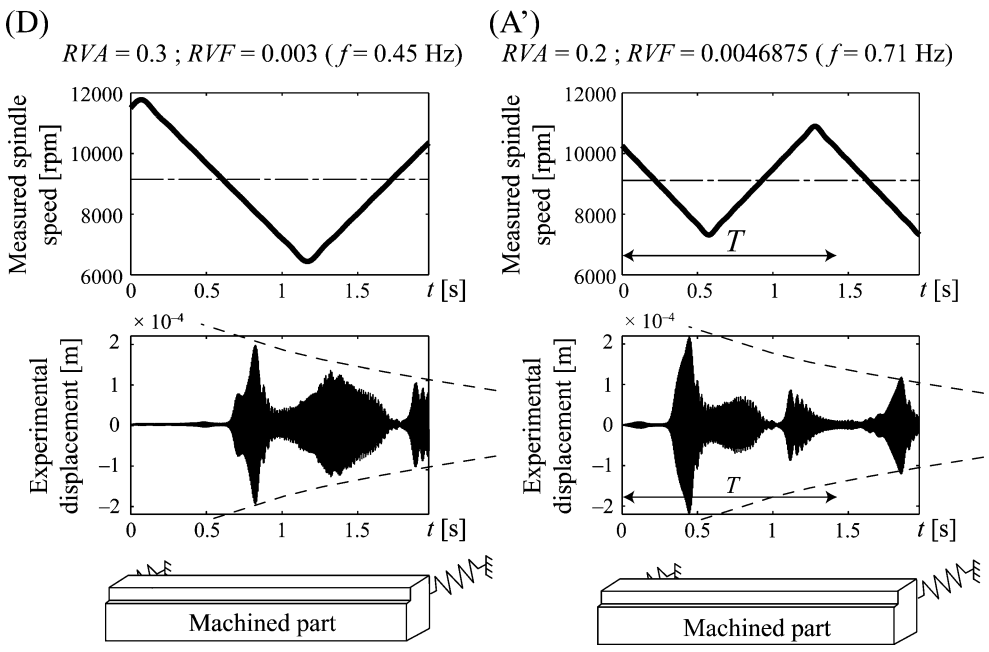

Fig. 13 Cutting test associated with points D and A' in Fig. 6 (A_p=2 mm and N_0=9,100 rpm)

Transient vibrations also occur for constant speed machining, but these decay within a few tooth passing period (note that for constant speed machining the principal period is the tooth passing period, τ_0).

7 Conclusions

Variable spindle speed machining was studied for high-speed milling at around the first Hopf and the first flip lobes. Stability properties were predicted using the semi-discretization method and confirmed by time domain simulations. Different combinations of the amplitude and the frequency of the speed modulation were analyzed in order to find the optimal technique to suppress chatter. It was found that the stability properties can always be improved (i.e., the critical depth of cut can always be increased) by spindle speed variation within the unstable domain of the first flip lobe, while there are some spindle speeds where spindle speed variation does not provide any essential gain. Amplitude was also shown to have a greater effect on the stability of the process than frequency.

Cutting tests were performed for certain spindle speeds in the flip domain in order to verify the theoretical predictions. The stabilizing effect of spindle speed variation was clearly verified experimentally; a period doubling chatter was suppressed by applying a proper spindle speed variation.

Some adverse cases were also discussed. The concept of stability for variable spindle speed machining was shown to differ slightly from that of constant spindle speed, since the principal period of the system is equal to the spindle variation period (or to its integer multiple) instead of the tooth passing period. If the machining process is unstable, but the development of chatter requires more time than the duration of the process, then it can be considered as "practically stable" machining. On the other hand, if the machining process is stable, but strong transient vibrations arise, then the process can be considered "practically unstable."

The efficiency of spindle speed variation can be increased by spindles capable of providing high acceleration. This would allow the use of a wider range of amplitudes and frequencies. Furthermore, the application of high modulation frequencies would decrease the principal period of the system—beneficial for the suppression of transient vibrations.

Acknowledgments This work was supported in part by the European Union Interreg IIIa AEROSFIN, by the Region Midi-Pyrénées Project "Complex workpiece machining in aeronautical context," by the János Bolyai Research Scholarship of the HAS, and by the HSNF under grant number OTKA K72911.

References

1. Tobias SA, Fishwick W (1958) Theory of regenerative machine tool chatter. Engineer 205:199–203, 238–239
2. Tlusty J (1986) Dynamics of high-speed milling. Trans ASME J Eng Ind 108:59–67
3. Altintas Y, Budak E (1995) Analytical prediction of stability lobes in milling. Ann CIRP 44:357–362
4. Smith S, Tlusty J (1993) Efficient simulation programs for chatter in milling. Ann CIRP 42:463–466
5. Davies MA, Pratt JR, Dutterer B, Burns TJ (2002) Stability prediction for low radial immersion milling. Trans ASME J Manuf Sci Eng 124:217–225
6. Insperger T, Mann BP, Stépán G, Bayly PV (2003) Stability of up-milling and down-milling, Part 1: alternative analytical methods. Int J Mach Tools Manuf 43:25–34
7. Campomanes ML, Altintas Y (2003) An improved time domain simulation for dynamic milling at small radial immersions. Trans ASME J Manuf Sci Eng 125:416–422
8. Bayly PV, Halley JE, Mann BP, Davies MA (2003) Stability of interrupted cutting by temporal finite element analysis. Trans ASME J Manuf Sci Eng 125:220–225
9. Merdol SD, Altintas Y (2004) Multi frequency solution of chatter stability for low immersion milling. Trans ASME J Manuf Sci Eng 126:459–466
10. Paris H, Peigné G, Mayer R (2004) Surface shape prediction in high speed milling. Int J Mach Tools Manuf 44:1567–1576
11. Solis E, Peres CR, Jiménez JE, Alique JR, Monje JC (2004) A new analytical–experimental method for the identification of stability lobes in high-speed milling. Int J Mach Tools Manuf 44:1591–1597
12. Surmann T, Enk D (2007) Simulation of milling tool vibration trajectories along changing engagement conditions. Int J Mach Tools Manuf 47:1442–1448
13. Seguy S, Campa FJ, López de Lacalle LN, Arnaud L, Dessein G, Aramendi G (2008) Toolpath dependent stability lobes for the milling of thin-walled parts. Int J Mach Machinabil Mater 4:377–392
14. Seguy S, Dessein G, Arnaud L (2008) Surface roughness variation of thin wall milling, related to modal interactions. Int J Mach Tools Manuf 48:261–274
15. Tlusty J, Smith S, Winfough WR (1996) Techniques for the use of long slender end mills in high-speed milling. Ann CIRP 4:393–396
16. Duncan GS, Tummond MF, Schmitz TL (2005) An investigation of the dynamic absorber effect in high-speed machining. Int J Mach Tools Manuf 45:497–507
17. Altintas Y, Engin S, Budak E (1999) Analytical stability prediction and design of variable pitch cutters. Trans ASME J Manuf Sci Eng 121:173–178
18. Budak E (2003) An analytical design method for milling cutters with nonconstant pitch to increase stability, Part I: theory. Trans ASME J Manuf Sci Eng 125:29–34
19. Stone BJ (1970) The effect on the chatter behaviour of machine tools of cutters with different helix angles on adjacent teeth. In: Proceedings of the 11th MTDR Conference, Macmillan pp 169–180
20. Sims ND, Mann BP, Huyanan S (2008) Analytical prediction of chatter stability for variable pitch and variable helix milling tools. J Sound Vib 317:664–686
21. Takemura T, Kitamura T, Hoshi T, Okushima K (1974) Active suppression of chatter by programmed variation of spindle speed. Ann CIRP 23:121–122

22. Sexton JS, Milne RD, Stone BJ (1977) A stability analysis of single point machining with varying spindle speed. Appl Math Model 1:310–318
23. Sexton JS, Stone BJ (1978) The stability of machining with continuously varying spindle speed. Ann CIRP 27:321–326
24. Sexton JS, Stone BJ (1980) An investigation of the transient effects during variable speed cutting. J Mech Eng Sci 22:107–118
25. Tsao TC, McCarthy MW, Kapoor SG (1993) A new approach to stability analysis of variable speed machining systems. Int J Mach Tools Manuf 33:791–808
26. Jayaram S, Kapoor SG, DeVor RE (2000) Analytical stability analysis of variable spindle speed machining. Trans ASME J Manuf Sci Eng 122:391–397
27. Insperger T, Stépán G (2004) Stability analysis of turning with periodic spindle speed modulation via semidiscretization. J Vib Control 10:1835–1855
28. Zhang H, Jackson MJ, Ni J (2009) Stability analysis on spindle speed variation method for machining chatter suppression. Int J Mach Machinabil Mater 5:107–128
29. Al-Regib E, Ni J, Lee SH (2003) Programming spindle speed variation for machine tool chatter suppression. Int J Mach Tools Manuf 43:1229–1240
30. Yang F, Zhang B, Yu J (2003) Chatter suppression with multiple time-varying parameters in turning. J Mater Process Technol 141:431–438
31. Sastry S, Kapoor SG, DeVor RE (2002) Floquet theory based approach for stability analysis of the variable speed face-milling process. Trans ASME J Manuf Sci Eng 124:10–17
32. Zatarain M, Bediaga I, Muñoa J, Lizarralde R (2008) Stability of milling processes with continuous spindle speed variation: analysis in the frequency and time domains, and experimental correlation. Ann CIRP 57:379–384
33. Altintas Y, Chan PK (1992) In-process detection and suppression of chatter in milling. Int J Mach Tools Manuf 32:329–347
34. Bediaga I, Egaña I, Muñoa J (2006) Reducción de la inestabilidad en cortes interrumpidos en fresado a alta velocidad mediante variación de la velocidad del husillo. In: XVI Congreso de Máquinas-Herramienta y Tecnologías de Fabricación, San Sebastián, Spain
35. Radulescu R, Kapoor SG, DeVor RE (1997) An investigation of variable spindle speed face milling for tool-work structures with complex dynamics, Part 2: physical explanation. Trans ASME J Manuf Sci Eng 119:273–280
36. Insperger T, Stépán G (2002) Semi-discretization method for delayed systems. Int J Numer Meth Eng 55:503–518
37. Lin SC, DeVor RE, Kapoor SG (1990) The effects of variable speed cutting on vibration control in face milling. Trans ASME J Eng Ind 112:1–11
38. Long XH, Balachandran B, Mann BP (2007) Dynamics of milling processes with variable time delays. Nonlinear Dynam 47:49–63
39. Faassen RPH, van de Wouw N, Nijmeijer H, Oosterling JAJ (2007) An improved tool path model including periodic delay for chatter prediction in milling. J Comput Nonlinear Dynam 2:167–179
40. Insperger T, Stépán G, Turi J (2008) On the higher-order semi-discretizations for periodic delayed systems. J Sound Vib 313:334–341
41. Mann BP, Insperger T, Stépán G, Bayly PV (2003) Stability of up-milling and down-milling, part 2: experimental verification. Int J Mach Tools Manuf 43:35–40